Top EFT prospects with differential spin observables

Liam Moore[1], based on 171X.XXXX *(to appear)*
with Andy Buckley[2] & Anna Duncan[2]

[1]CP3 Louvain-la-Neuve
[2]ATLAS, University of Glasgow

2017 HL-LHC Workshop, CERN

Motivations

The large top mass $m_t \sim 173\,\text{GeV} \leftrightarrow y_t \sim 1$ in the SM $\iff$ $\mathbf{t} \heartsuit \mathbf{H}$

- t-quark chief troublemaker creating hierarchy problem. Naturalness: if NP stabilizes EW scale, should expect that BSM is t-philic
- $m_t > m_W + m_b \implies \Gamma_t \gg \Lambda_{\text{QCD}}$. Decay rate $>$ hadronisation timescale, so spin information preserved in decay products.
- Measuring angular distributions gives additional information on production/decay mechanism, sensitive to $\mathcal{P}, \mathcal{CP} \ldots$
- (HL-)LHC: $\sim 3 \times 10^9$ $t\bar{t}$ pairs at $4ab^{-1}$. Both precision and a wide array of differential measurements possible.

Question:

What are the prospects for constraining sources of NP, in differential distributions sensitive to t-polarisation and spin-correlations?

Non-resonant BSM with the SMEFT

The future divides into two possibilities:

- $\sqrt{s}_{\text{LHC}} \geq \Lambda_{\text{NP}}$: resonances accessible, measure properties
- $\sqrt{s}_{\text{LHC}} < \Lambda_{\text{NP}}$: states decoupled, observe only off-shell effects

Latter case: construct general gauge-invariant $\mathcal{L}_{\text{SMEFT}}$ from operators at each order in $1/\Lambda_{\text{NP}}$, constrain NP in contact interactions $\propto {}^{C_i}/_{\Lambda^2}$:

$$\mathcal{L}_{\text{SMEFT}} \equiv \mathcal{L}^{(4)}_{\text{SM}}(\{\Phi_{\text{SM}}\}) + \frac{C_i}{\Lambda^{d-4}} \mathcal{O}^{(d)}_i(\{\Phi_{\text{SM}}\}) + \ldots$$

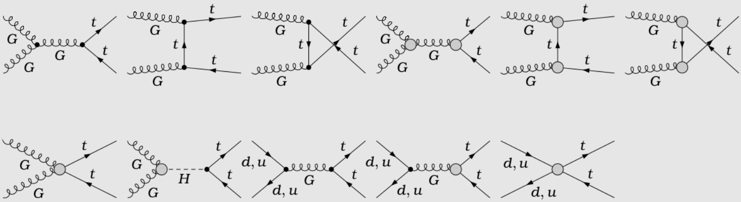

An example: new physics in $t\bar{t}$ production

Coefficient C_i	Operator $\mathcal{O}_i$
C_G	$f_{ABC}G_\mu^{A\nu}G_\nu^{B\lambda}G_\lambda^{C\mu}$
C_{uG}^{33}	$(\bar{q}\sigma^{\mu\nu}T^A u)\tilde{\varphi}G_{\mu\nu}^A$
$C_{qq}^{(1)}$	$(\bar{q}\gamma_\mu q)(\bar{q}\gamma^\mu q)$
$C_{qq}^{(3)}$	$(\bar{q}\gamma_\mu \tau^I q)(\bar{q}\gamma^\mu \tau^I q)$
C_{uu}	$(\bar{u}\gamma_\mu u)(\bar{u}\gamma^\mu u)$
$C_{qu}^{(8)}$	$(\bar{q}\gamma_\mu T^A q)(\bar{u}\gamma^\mu T^A u)$
$C_{qd}^{(8)}$	$(\bar{q}\gamma_\mu T^A q)(\bar{d}\gamma^\mu T^A d)$
$C_{ud}^{(8)}$	$(\bar{u}\gamma_\mu T^A u)(\bar{d}\gamma^\mu T^A d)$

Table: $\mathcal{O}_i$ $(pp \to t\bar{t})$: viable UV models

EFT can constrain multiple BSM models simultaneously:

- Heavy coloured fermions, technihadrons. . .
- Compositeness, stops, 2HDM. . .
- W' & Z's
- Heavy (axi)gluons. . .
- Allow all $\mathcal{O}_i$ simultaneously $\Longrightarrow$ **global fit (1512.03360)**

TopFitter: use parton-level top measurements to extract marginalised constraints on C_i in (primarily) $t\bar{t}$ + single-t production.

TopFitter v1.0 at a glance - Global 95% C.I.

- Limits 'weak': **weakly coupled UV unconstrained**!
- Partonic distributions $\Longrightarrow$ see only 4 l.c. of 6 ψ^4 operators
- One route to improvement: include distributions of decay products $\Longrightarrow$ probe $t\bar{t}$ spins
- Sensitive to $\mathcal{P}, \mathcal{CP}$-odd $\mathcal{O}_i$, break ψ^4 degeneracies, derive complementary bounds. . .
- Requires comparing distributions at the particle level

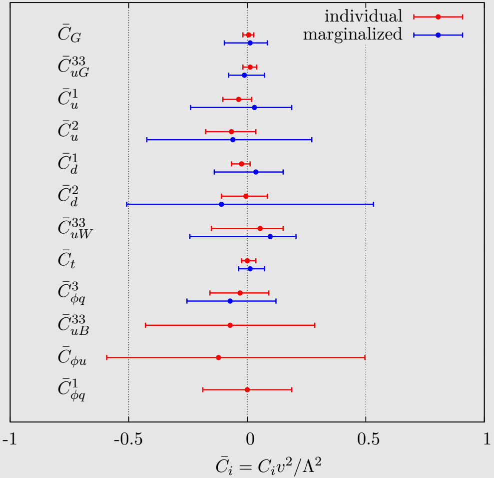

Inferring $t\bar{t}$ spins from decay modes

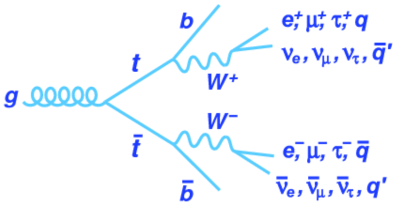

Figure: $t\bar{t}$ decay modes

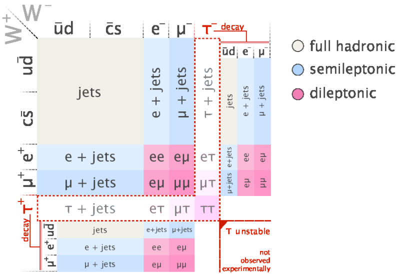

Figure: Credit: Nazar Bartosik

Left-handed decay $\implies$ spin aligned with l/d direction in t-rest frame.

Use $l^{\pm}$/light jet three-momentum as proxy to top spin. 2 options:

- Semileptonic: $BR \sim 30\%$, but $\alpha_i^{\text{jet}} \sim 50\%\ \alpha_i^d \equiv \hat{s} \cdot \hat{p}_d \simeq 1$
- Dileptonic: $BR \sim 5\%, \alpha_i \simeq 1, 2 \times \nu \implies$ reconstruction harder

The $t\bar{t}$ spin-density matrix

$\mathcal{M}^{*\,\alpha'\beta'}_{xy\to t\bar{t}}\,\mathcal{M}^{\alpha\beta}_{xy\to t\bar{t}}$ with $t, \bar{t}$ spin indices explicit $\equiv$ $t\bar{t}$ **spin density matrix**

$$R^{t\bar{t}} \propto \left[A^I\, \mathbb{1}\otimes\mathbb{1} + \tilde{B}^+_i\, \sigma^i \otimes \mathbb{1} + \tilde{B}^-_i\, \mathbb{1}\otimes\sigma^i + \tilde{C}_{ij}\,\sigma^i\otimes\sigma^j\right]$$

NP $\Leftrightarrow$ $\mathbf{C_i}$ **contribute to functions** $\mathbf{A}, \mathbf{B_i}, \mathbf{C_{i\,j}}$ appropriately

This information is propagated through the W-decay to the distributions:

$$\frac{1}{\sigma}\frac{\mathrm{d}^2\sigma}{\mathrm{d}\Omega_+\mathrm{d}\Omega_-} = \frac{1}{(4\pi)^2}\left(1 + \mathbf{B}_1'\cdot\hat{\ell}_+ + \mathbf{B}_2'\cdot\hat{\ell}_- - \hat{\ell}_+\cdot C'\cdot\hat{\ell}_-\right)$$

Choosing basis for spin axes $\Longleftrightarrow$ isolate $\mathcal{O}$'s in particular angular distributions. **(Bernreuther et al 1508.05271)** proposed $i, j = \{\hat{\mathbf{r}}, \hat{\mathbf{k}}, \hat{\mathbf{n}}\}$.

6+9 $\cos\theta_i^{\pm}$ distributions probe sources of polarisation+spin correlations

Each B, C has **dependence on kinematics** $\propto$ operator coefficients

CMS: $\cos\theta_k^{\pm}$ (1601.01107)

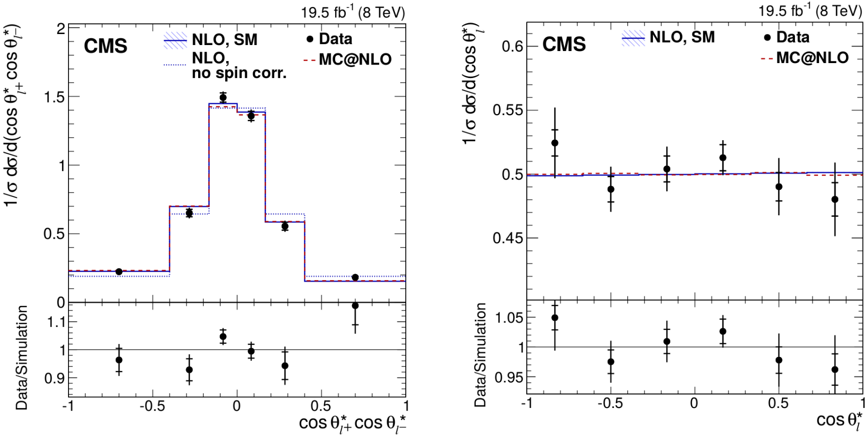

Unfolded 8TeV measurements of $\cos\theta_k^{\pm}$ distributions, probing spin correlations $C(k,k)$ (left) and polarisation coefficients $B(k)$ (right)

ATLAS: $\cos\theta^{\pm}_{r/k}$ (1612.07004)

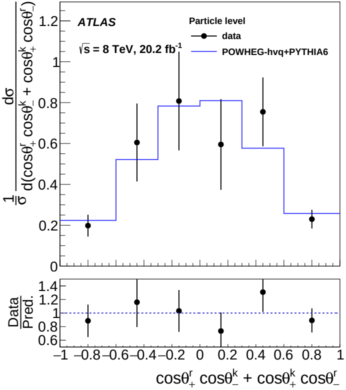

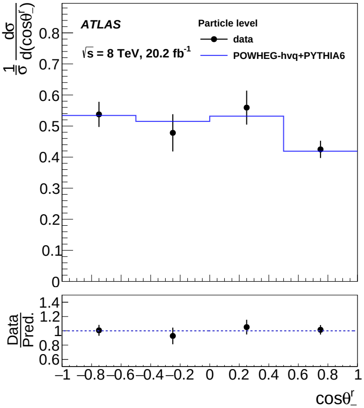

8TeV particle-level reconstructed distributions for $\cos\theta^{\pm}_{r/k}$ sensitive to spin correlations $C(r,k)$ (left), and polarisation coefficients $B(r)$ (right)

Studying the sensitivity of spin observables

	NLO+EW	$\propto \hat{\mu}_t$
$C(r,\ r)$	$0.071^{+0.008}_{-0.006}$	$2.475^{+0.020}_{-0.019}$
$C(k,\ k)$	$0.331^{+0.002}_{-0.002}$	$0.917^{+0.006}_{-0.006}$
--	--	$\propto \hat{c}_{VA}$
$B_{1/2}(r)$	$(3.2^{+2.3}_{-1.7}) \cdot 10^{-3}$	$0.210^{+0.009}_{-0.009}$
$B_{1/2}(k)$	$(8.0^{+3.4}_{-2.4}) \cdot 10^{-3}$	$1.607^{+0.051}_{-0.052}$

Table: Numerical sensitivity of obs $\propto \hat{c}$ (parton-level). Errors: $\mu = m_t/2 \leftrightarrow 2m_t$ **(Bernreuther et al 1508.05271, 1003.3926)**

$$\mathcal{O}_{\text{CMDM}} = -\frac{g_s}{2m_t}\hat{\mu}_t \bar{t}\sigma^{\mu\nu}T^a t G^a_{\mu\nu}$$

$$\mathcal{O}_{VA} = \frac{g_s^2}{2m_t^2}\hat{c}_{VA}(\bar{q}\gamma^\mu T^a q)(\bar{t}\gamma_\mu\gamma_5 T^a t)$$

- Pick two representative operators that modify Bs and Cs for given axes
- Parton-level expectations modified by shower, acceptance cuts, reconstruction. . .
- Overlap with global fit: compare sensitivity of spin vs. kinematic distributions
- Double differential: resolve $m_{t\bar{t}}$ dependence, enhance NP. Gains?

Analysis Summary

Leptons	$p_T > 25$ GeV
	$\lvert\eta\rvert < 2.5$
Jets	anti-k_T $R = 0.4$
	$p_T > 25$ GeV , $\lvert\eta\rvert < 2.5$
	b-tag w/ 70% efficiency
	1% fake rate w/ FastJet
Reconstruction	Pair b jets, $l^{\pm}$ using M_{T2}
	ν solutions w/ MAOS
	(Cho et al. 0810.4853)
Require	≥ 2 jets w/ ≥ 1 b-tags
	$\geq 1 \times l^+, l^-$

Table: Event selection criteria in Rivet analysis

- ME+decays: FeynRules+UFO+MG5_aMCNLO
- Shower: Pythia8+UMEPS
- Analysis: Rivet+YODA
- Rescale σ_{incl} with NNLO k-factor **(Czakon et al 2013)**
- Attach μ to extrapolate D6 to different $\hat{c}$ values (to $\mathcal{O}(\Lambda^{-2})$)
- Construct binned log-likelihood, exclude $\hat{c}$ for $CL_s < 0.05$ assuming SM for toy $\mathcal{L}_{\text{int}}$, ϵ_{syst}

$\cos\theta_\pm$ polarisation distributions - $c_{\hat{VA}}$ vs SM

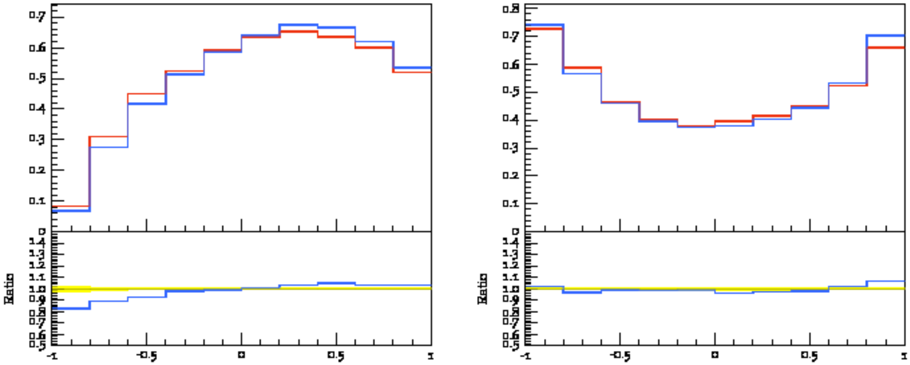

Left (Right): Reconstructed $\frac{1}{\sigma}\frac{d\sigma}{d(\cos\theta^+_{k(r)})}$ distributions for the SM and $c_{\hat{VA}} = 0.25$ sensitive to $\mathbf{B_k}$ $(\mathbf{B_r})$.

2D $\cos\theta_{\pm}$ polarisation distributions - $c_{\hat{VA}}$ vs SM

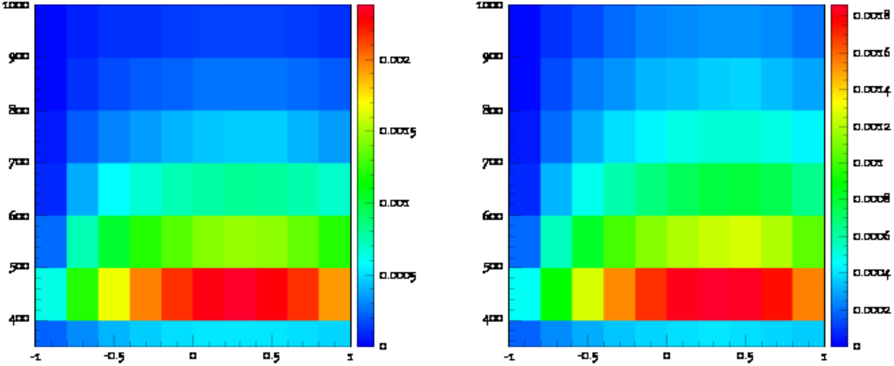

Left (Right): Reconstructed $\frac{1}{\sigma}\frac{d^2\sigma}{dm_{t\bar{t}}d(\cos\theta^{+}_{k(r)})}$ distributions for the SM ($c_{\hat{VA}} = 0.25$) sensitive to $\mathbf{B_k}$ $(\mathbf{B_r})$.

$\cos\theta_+ \cos\theta_-$ spin correlation distributions - $\hat{\mu}_t$ vs. SM

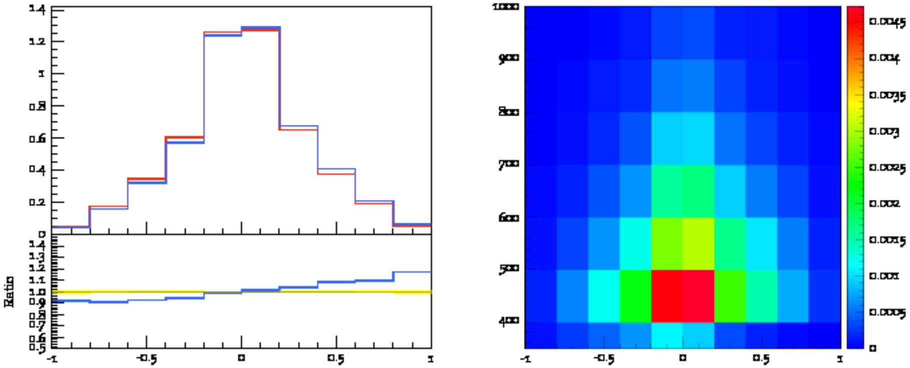

Left (Right): $\dfrac{d\sigma}{d(\cos\theta_n^+ \cos\theta_n^-)}$ $\left(\dfrac{1}{\sigma}\dfrac{d^2\sigma}{dm_{t\bar{t}}d(\cos\theta_n^+ \cos\theta_n^-)}\right)$ for the SM, $\hat{\mu}_t = 0.05$. Sensitive to $\mathbf{C_{nn}}$.

$\hat{\mu}_t$: 1D $\cos\theta_n^+ \cos\theta_n^-$

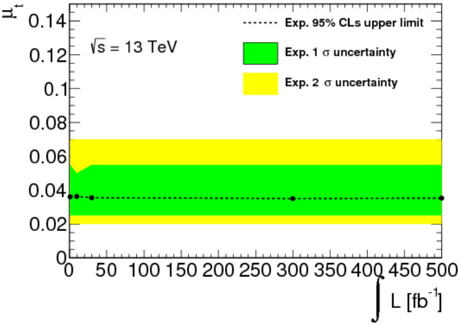

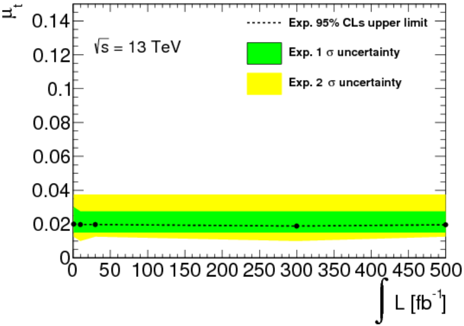

Expected exclusion limits from $\frac{d\sigma}{d(\cos\theta_n^+ \cos\theta_n^-)}$ with $\epsilon_{\text{syst}} = 10\%, 5\%$

$$-0.053 < \hat{\mu}_t < 0.042 \text{ CMS, 8TeV } \textbf{(1601.01107)}$$

1D differential **syst. dominated**, comparable results to 8TeV CMS limit

$\hat{\mu}_t$: 1D $m_{t\bar{t}}$ distribution vs. $\cos\theta_k^+ \cos\theta_k^-$

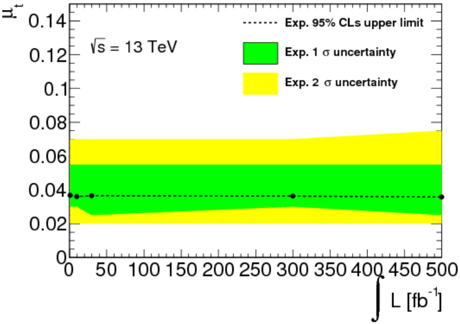

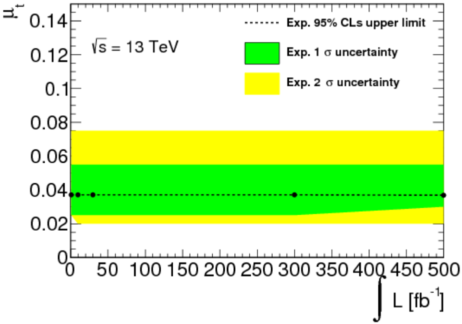

Exclusion limits from $\frac{d\sigma}{dm_{t\bar{t}}}$ and $\frac{d\sigma}{d(\cos\theta_k^+ \cos\theta_k^-)}$ respectively, $\epsilon_{\text{syst}} = 10\%$

$-0.068 < \hat{\mu}_t < 0.029$ TopFitter w/ 8TeVp_T spectra **(1607.04304)**

Numerically **similar results for** r, k **and** n **correlations**. Spin $\sim$ kinematic.

$\hat{\mu}_t$: 1D vs 2D $\cos\theta_k^+ \cos\theta_k^-$ distributions

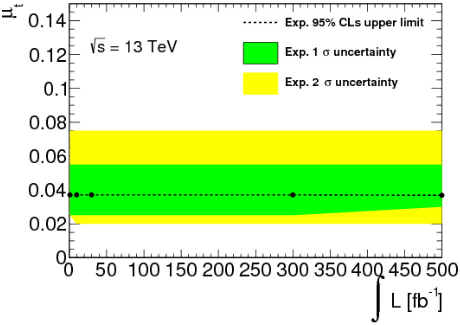

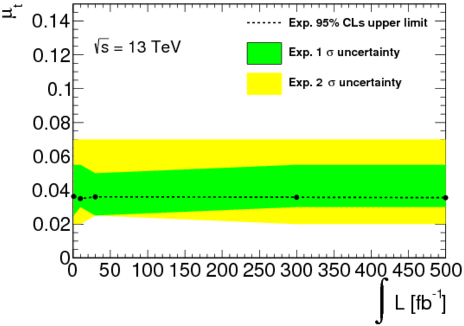

Exclusion limits for $\dfrac{d^{(2)}\sigma}{d\cos\theta_k^+ \cos\theta_k^- \,(dm_{t\bar{t}})}$ 1D vs 2D respectively, $\epsilon_{\text{syst}} = 10\%$

$\hat{\mu}_t$ marginal $(\mathcal{O}(5\%))$ gains from resolving $m_{t\bar{t}}$ dependence of spin correlations. 2D improves with L_{int} at similar level.

D5: weaker scaling. k-axes spin correlations degrade w/ $m_{t\bar{t}}$ c.f. QCD.

$\hat{c}_{VA}$: 1D $\cos\theta_r^+$ vs. $\cos\theta_k^+$

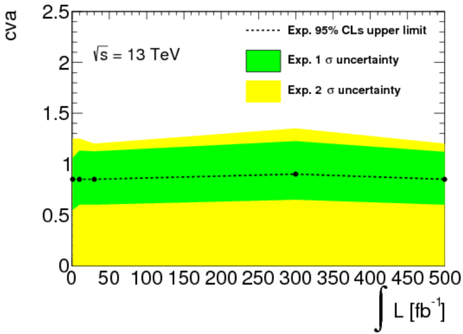

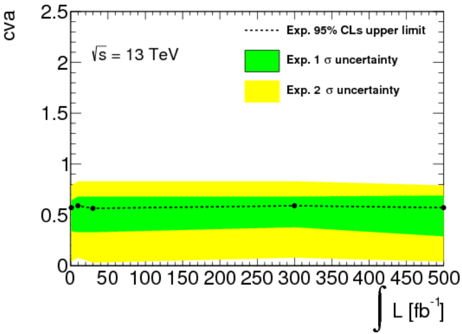

Exclusion limits from $\frac{d\sigma}{d\cos\theta_r}$ and $\frac{d\sigma}{d\cos\theta_k}$ respectively, $\epsilon_{\text{syst}} = 10\%$

Unconstrained in kinematic distributions, typical TopFitter ψ^4 limits $\hat{c} \lesssim 0.2$

Sensitivity hierarchy $B(k) > B(r)$ follows parton level expectation

$\hat{c}_{VA}$: 1D vs 2D $\cos\theta_k^+$ distributions

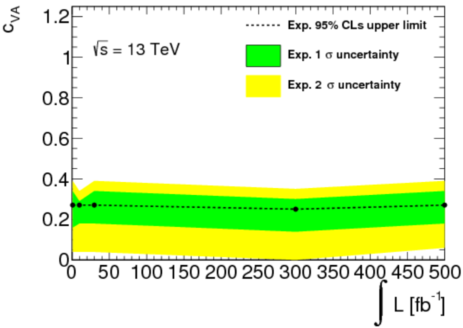

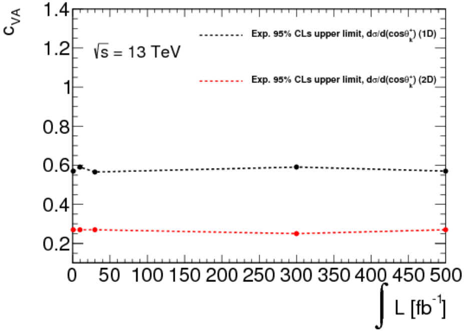

Exclusion limits from $\frac{d^2\sigma}{dm_{t\bar{t}}d\cos\theta_k^+}$ and 1D vs 2D respectively, $\epsilon_{\text{syst}} = 10\%$

$\mathcal{O}\left(\Lambda^{-4}\right)$ effects start to become significant for $m_{t\bar{t}} > 1\text{TeV}$.

Here: even cutting bins $m_{t\bar{t}} < 1\text{TeV}$, factor $\geq$ 2 improvement 1D $\rightarrow$ 2D.

Improves w/ L_{int} for $m_{t\bar{t}} > 1\text{TeV}$ region, but require EFT uncertainties.

Summary & Outlook

From preliminary results:

- 1D spin $\sim$ kinematic, syst. dominated, limits consistent with TopFitter
- Bound unconstrained ψ^4 operators at comparable level
- Double-differential: naively improve ψ^4 by factor ~ 2
- Improvements with L_{int} req. lowering systematics below 10% level

Several directions for improvement:

- NLO+MadSpin $\longrightarrow$ differential SM NLO k-factors + theory uncertainties
- Quantify EFT uncertainties in typical power counting scenarios
- Investigate quadratic EFT contributions to observables. . .
- Compare against lepton + jets, for all operators. . .

Contents

TopFitter v1.0 - Overview

Idea: perform a simultaneous fit of the $(\mathcal{CP}-\text{even})$ operators affecting (single + pair) top production and decay observables. In a nutshell:

- Use FeynRules/MadGraph5_aMC@NLO/MadAnalysis toolchain, sample observables at fixed points in $\{C_i\}$ space
- Approximate linear dep. of observables on $C_i \implies$ use polynomial interpolation method (Professor) to fill parameter space
- Perform a χ^2 fit using this and publicly available LHC and TeVatron (differential and rate) measurements

Goals: Search for non-resonant NP signals, identify and understand sensitivity to operators, compare limits with resonance searches, establish feasibility of 9+ dimensional fit. . .

Backup: TopFitter Setup (I)

- MadGraph+UFO observables supplemented by approximate NLO QCD corrections, modelled by differential SM-only $k-$factors generated with MCFM and verified with aMC_@NLO
- Theory uncertainties estimated by independently varying $\mu_{\text{central}}/2 < \mu_{\mathrm{R,F}} < 2\mu_{\text{central}}$, $\mu_{\text{central}} = m_t$.
- PDF uncertainties were estimated by generating events using the NLO NNPDF23, MSTW2008, and CT10 PDF sets, according to the PDF4LHC prescription.
- For top pair total inclusive cross-sections we used global K-factors from NNLO QCD with soft gluons resummed to NNLL accuracy

Central value taken as estimate and the **width of the envelope** (including scale variations) as the total theoretical uncertainty.

Backup: TopFitter Setup (II)

- Total of 195 measurements, predominantly Run I LHC $t\bar{t}$, single top (differential) cross sections, but also A_{FB}, A_{C}, Γ_{top} and $W-$helicity fractions and $\sigma_{t\bar{t}V}$
- Measurements included quoted in terms of parton-level unfolded quantities (far more abundant, computationally less expensive)
- Experimental uncertainties (stat, syst, lumi) included as quoted, correlations between bins from unfolding included wherever quoted (otherwise assumed to be uncorrelated)
- Interpolated $f_b(\{C_i\}) = \alpha_0^b + \sum_i \beta_i^b C_i + \sum_{i\leq j} \gamma_{i,j}^b C_i C_j + \ldots$ introduces parametrisation error $\lesssim 5\%$ from explicit MC
- Confidence intervals constructed from minimizing χ^2/d.o.f. allowing all C_i to vary (marginalized), or each to vary individually

TopFitter v1.0 - Datasets

Dataset	$\sqrt{s}$ (TeV)	Measurements	arXiv ref.	Dataset	$\sqrt{s}$ (TeV)	Measurements	arXiv ref.
Top pair production							
Total cross-sections:				Differential cross-sections:			
ATLAS	7	lepton+jets	1406.5375	ATLAS	7	$p_T(t), M_{t\bar{t}}, \|y_{t\bar{t}}\|$	1407.0371
ATLAS	7	dilepton	1202.4892	CDF	1.96	$M_{t\bar{t}}$	0903.2850
ATLAS	7	lepton+tau	1205.3067	CMS	7	$p_T(t), M_{t\bar{t}}, y_t, y_{t\bar{t}}$	1211.2220
ATLAS	7	lepton w/o b jets	1201.1889	CMS	8	$p_T(t), M_{t\bar{t}}, y_t, y_{t\bar{t}}$	1505.04480
ATLAS	7	lepton w/ b jets	1406.5375	DØ	1.96	$M_{t\bar{t}}, p_T(t), \|y_t\|$	1401.5785
ATLAS	7	tau+jets	1211.7205				
ATLAS	7	$t\bar{t}, Z\gamma, WW$	1407.0573	Charge asymmetries:			
ATLAS	8	dilepton	1202.4892	ATLAS	7	A_C (inclusive+$M_{t\bar{t}}, y_{t\bar{t}}$)	1311.6742
CMS	7	all hadronic	1302.0508	CMS	7	A_C (inclusive+$M_{t\bar{t}}, y_{t\bar{t}}$)	1402.3803
CMS	7	dilepton	1208.2761	CDF	1.96	A_{FB} (inclusive+$M_{t\bar{t}}, y_{t\bar{t}}$)	1211.1003
CMS	7	lepton+jets	1212.6682	DØ	1.96	A_{FB} (inclusive+$M_{t\bar{t}}, y_{t\bar{t}}$)	1405.0421
CMS	7	lepton+tau	1203.6810				
CMS	7	tau+jets	1301.5755	Top widths:			
CMS	8	dilepton	1312.7582	DØ	1.96	Γ_{top}	1308.4050
CDF + DØ	1.96	Combined world average	1309.7570	CDF	1.96	Γ_{top}	1201.4156
Single top production				W-boson helicity fractions:			
ATLAS	7	t-channel (differential)	1406.7844	ATLAS	7		1205.2484
CDF	1.96	s-channel (total)	1402.0484	CDF	1.96		1211.4523
CMS	7	t-channel (total)	1406.7844	CMS	7		1308.3879
CMS	8	t-channel (total)	1406.7844	DØ	1.96		1011.6549
DØ	1.96	s-channel (total)	0907.4259				
DØ	1.96	t-channel (total)	1105.2788				
Associated production				*Run II data*			
ATLAS	7	$t\bar{t}\gamma$	1502.00586	CMS	13	$t\bar{t}$ (dilepton)	1510.05302
ATLAS	8	$t\bar{t}Z$	1509.05276				
CMS	8	$t\bar{t}Z$	1406.7830				

NP in angular distributions

Fix (an arbitrary) set of axes along which to quantize the $t\bar{t}$ spins. Each contribution then isolated in the 1D distributions:

$$\frac{1}{\sigma}\frac{d\sigma}{d\cos\theta_\pm} = \frac{1}{2}\left(1 + B_{1,2}\,\cos\theta_\pm\right)$$

$$\frac{1}{\sigma}\frac{d\sigma}{d\xi_{ab}} = \frac{1}{2}\left(1 - C\xi\right)\,\ln\left(\frac{1}{|\xi_{ab}|}\right)\,,\xi_{ab} = \cos\theta_+\,\cos\theta_-$$

$$\hat{\mathbf{r}}_p = \frac{1}{r_p}(\hat{\mathbf{p}}_p - y_p\hat{\mathbf{k}})\,,\quad \hat{\mathbf{k}} \equiv \hat{t}_{\text{ZMF}}\,,\quad \hat{\mathbf{n}}_p = \frac{1}{r_p}(\hat{\mathbf{p}}_p \times \hat{\mathbf{k}})\,,y_p = \hat{\mathbf{p}}_p.\hat{\mathbf{k}}$$

with $\cos\theta^\pm$ measured with respect to the axes $\hat{\mathbf{a}}$, $\hat{\mathbf{b}} = \hat{\mathbf{r}}, \hat{\mathbf{k}}, \hat{\mathbf{n}}$.

Each B, C contains dependence on $t\bar{t}$ kinematics $\propto$ operator coefficients. c.f. in QCD, spin-correlations along $\hat{\mathbf{k}}$ degrade for high $m_{t\bar{t}}$.

Operators $\leftrightarrow$ observables

Correlation	$\mathcal{CP}$-properties	sensitive to
$B_1(r) + B_2(r)$	$\mathcal{P}$-odd, $\mathcal{CP}$-even	$\hat{\mathbf{c}}_{\mathbf{VA}}, \hat{c}_3$
$B_1(k) + B_2(k)$	$\mathcal{P}$-odd, $\mathcal{CP}$-even	$\hat{\mathbf{c}}_{\mathbf{VA}}, \hat{c}_3$
$C(n,\ n)$	$\mathcal{P}$-, $\mathcal{CP}$-even	$\hat{c}_{VV}, \hat{c}_1, \hat{\mu}_{\mathbf{t}}$
$C(r,\ r)$	$\mathcal{P}$-, $\mathcal{CP}$-even	$\hat{c}_{VV}, \hat{c}_1, \hat{\mu}_{\mathbf{t}}$
$C(k,\ k)$	$\mathcal{P}$-, $\mathcal{CP}$-even	$\hat{c}_{VV}, \hat{c}_1, \hat{\mu}_{\mathbf{t}}$
$C(r,\ k) + C(k,\ r)$	$\mathcal{P}$-, $\mathcal{CP}$-even	$\hat{c}_{VV}, \hat{c}_1, \hat{\mu}_{\mathbf{t}}$

Subset of correlation coefficients in **(Bernreuther et al 1508.05271)**. Angular distributions w.r.t. axes $(r, k, n \ldots)$ probe different $\mathcal{O}_i$.

- Each distribution is sensitive to subset of $t\bar{t}$ dimension-six operators.
- Here we'll pick one each for the polarisation angle and spin-correlation distributions.

Consequences of EFT Validity

- Strength of constraints $\iff$ range of EFT validity
- Match $\frac{C_i}{\Lambda^2} = \frac{g_*^2}{M_*^2}$
- Impose $M_* > \kappa\Lambda > m_{t\bar{t}}^{\text{max}}$
- Weak constraint $\implies$ larger g_*, higher-order corrections to BSM important
- Truncation at e.g. $\mathcal{O}(\Lambda^{-2})$ less reliable

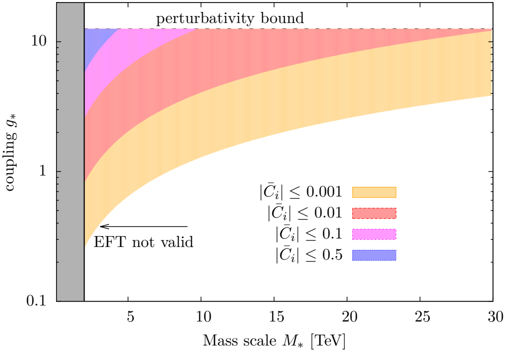

Figure: Areas in the $g_* - M_*$ plane. Coloured areas constrained in perturbative models subject to condition $C/\Lambda^2 = g_*^2/M_*^2$. Shaded grey area: mass scales $M_* < m_{t\bar{t}}^{\text{max}}$

Limit-setting

- We use log-likelihood ratio $q = -2\log(\frac{\mathcal{L}_1}{\mathcal{L}_0})$ as test statistic
- Systematic uncertainties simulated as flat $\%$ gaussian uncertainty on the background imposed on all bins
- Theory uncertainties not represented here (yet) ($\sim$ negligible in (1D) measurements). Flat NNLO k-factor **(Czakon et al 2013)**.
- Build up LLR p.d.f.s under $f_{0/1}(q)$ for SM and SM+D6 respectively
- Can form confidence intervals $CL_{(s+)b} = \int_{LLR_{obs}}^{\infty} f_{(1)0}(q)dq$ assuming observe SM expectation
- Exclude μ at 95$\%$ confidence level $\iff$ $CL_s = \frac{CL_{s+b}}{CL_b} < 0.05$

1D vs 2D LLRs: $\hat{\mu}_t$, 5%syst, $100fb^{-1}$

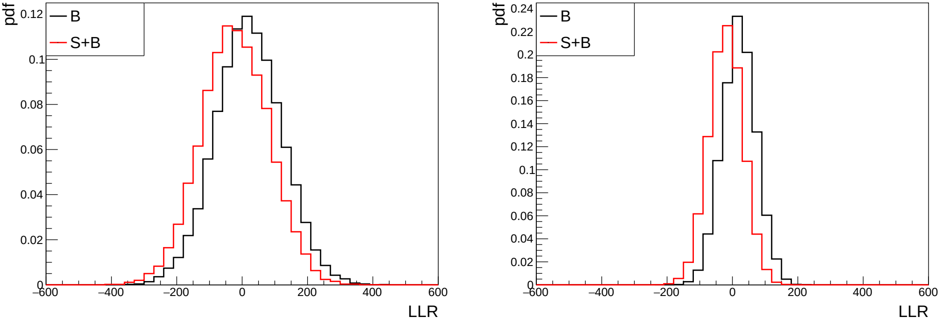

Left (Right): 1D (2D) LLR distributions for ξ_{kk} distribution in **SM** and **D6 EFT**. Smaller overlap between the distributions signifies 2D observables discriminate signal from background.